A remote sensing derived data set of 100 million individual tree crowns for the National Ecological Observatory Network

Ben. G. Weinstein¹ Sergio Marconi¹, Stephanie Bohlman², Alina Zare³, Aditya Singh⁴, Sarah J. Graves⁵, Ethan White¹

¹Department of Wildlife Ecology and Conservation, University of Florida, Gainesville, Florida, USA

²School of Forest Resources and Conservation, University of Florida, Gainesville, Florida, USA

³Department of Electrical and Computer Engineering, University of Florida, Gainesville, Florida, USA

⁴Department of Agricultural & Biological Engineering, University of Florida, Gainesville, FL 32611, USA

⁵ Nelson Institute for Environmental Studies, University of Wisconsin-Madison, Madison, Wisconsin, USA

Abstract

Forests provide essential biodiversity, ecosystem and economic services. Information on individual trees is important for understanding the state of forest ecosystems, but obtaining individual-level data at broad scales is challenging due to the costs and logistics of data collection. While advances in remote sensing techniques allow surveys of individual trees at unprecedented extents, there remain significant technical and computational challenges in turning sensor data into tangible information. Using deep learning methods, we produced an open-source dataset of individual-level crown estimates for 100 million trees at 37 sites across the United States surveyed by the National Ecological Observatory Network's Airborne Observation Platform. Each canopy tree crown is represented by a rectangular bounding box and includes information on the height, crown area, and spatial location of the tree. Tree crowns identified using this technique correspond well with hand-labeled crowns, exhibiting both high levels of overlap and good correspondence in height estimates. These data have the potential to drive significant expansion of individual-level research on trees by facilitating both regional analyses at scales of ~10,000 ha and cross-region comparisons encompassing forest types from most of the United States.

Introduction

Trees are central organisms in maintaining the ecological function, biodiversity and the health of the planet. There are estimated to be over three trillion individual trees on earth [1] covering a broad range of environments and geography [2]. Counting and measuring trees is central to developing an understanding of key environmental and economic issues and has implications for global climate, land management and wood production. Field-based surveys of trees are generally conducted at local scales (~0.1-100 ha) with measurements of attributes for individual trees within plots collected manually. Connecting these local scale measurements at the plot level to broad scale patterns is challenging because of spatial heterogeneity in forests. Many of the key processes in forests, including change in forest structure and function in response to disturbances such as hurricanes and pest outbreaks, and human modification through forest management and fire, occur at scales beyond those feasible for direct field measurement.

Satellite data with continuous global coverage have been used to quantify important patterns in forest ecology and management such as global tree cover dynamics and disturbances in temperate forests (e.g. [3]). However, the spatial resolution of satellite data makes it difficult to detect and monitor individual trees that underlie large scale patterns. These shortcomings can however be overcome by utilizing higher resolution remotely sensed data from low Earth orbit satellites, aircraft or drones to capture individual-level changes in forest structure and composition [4,5]. These high resolution data have become increasingly accessible, but converting the data into information on individual trees requires significant technical expertise and access to high-performance computing environments. This prevents most ecologists, foresters, and managers from engaging with large scale data on individual trees, despite the availability of the underlying data products and broad importance for forest ecology and management.

In response to the growing need for publicly-available and standardized airborne remote sensing data over forested ecosystems, the National Ecological Observatory Network (NEON) is collecting multi-sensor data for more than 40 forested sites across the US. In this research, we combine this data with a semi-supervised deep learning approach [6,7] to produce a dataset on the location, height and crown area of over 100 million individual canopy trees at 37 sites distributed across the United States. To make these data readily accessible, we are releasing easy to access data files to spur biological analyses and to facilitate model development for tasks that rely on individual tree prediction. We describe the components of this open-source dataset, compare predicted crowns with hand-labeled crowns for a range of forest types, and discuss how this dataset can be used to address key questions in forest research.

The NEON Crowns dataset

The NEON Crowns dataset contains tree crowns for all canopy trees (those visible from airborne remote sensing) at 37 NEON sites. Since subcanopy trees are not visible from above, they are not included in this dataset. We operationally define "trees" as plants over 3m tall. The 37 NEON sites represent all NEON sites containing trees with coregistered RGB and LiDAR data from 2018 or 2019 (see S3 for a list of sites and their locations). Predictions were made using the most recent year for which images were available for each site.

The dataset includes a total of 104,675,304 million crowns. Each predicted crown includes data on the spatial position of the crown bounding box, the area of the bounding box (an approximation of crown area), the 99th quantile of the height of LiDAR returns within the bounding box above ground level (an estimate of tree height), the year of sampling, the site where the tree is located, and a confidence score indicating the model confidence that the box represents a tree. The confidence score can vary from 0-1, but based on results from [6], boxes with less than 0.15 confidence were not included in the dataset.

The dataset is provided in two formats: 1) as 11,000 individual polygons (geospatial 'shapefiles' in standard ESRI™ format) each covering a single 1km^2 tile; and 2) as 37 csv files, each covering an entire NEON site. Geospatial tiles have embedded spatial projection information and can be read in commonly available GIS software (e.g., ArcGIS, QGIS) and geospatial packages for most common programming languages used in data analysis (e.g., R, Python). All data are publicly available, openly licensed (CC-BY), and permanently archived on Zenodo (https://zenodo.org/deposit/3765872).

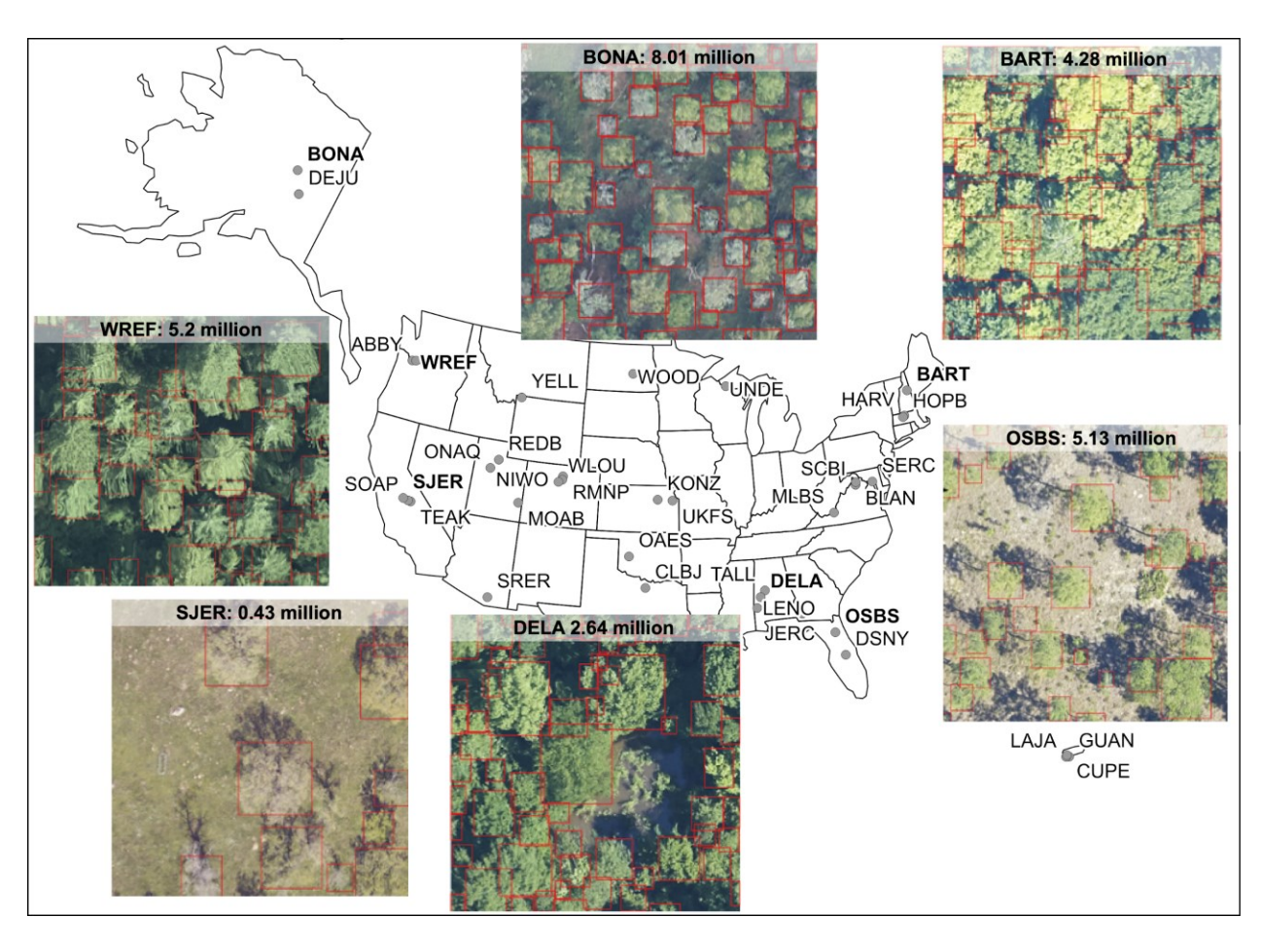


Figure 1. Locations of 37 NEON sites included in the NEON Crowns Dataset and examples of tree predictions shown with RGB imagery for six sites. Clockwise from bottom right: 1) OSBS: Ordway-Swisher Biological Station, Florida 2) DELA: Dead Lake, Alabama, 3) SJER: San Joaquin Experimental Range, California, 4) WREF: Wind River Experimental Forest,

Washington, 5) BONA: Caribou Creek, Alaska and 6) BART: Bartlett Experimental Forest, New Hampshire. Each predicted crown is associated with the spatial position, crown area, maximum height estimate from co-registered LiDAR data, and a predicted confidence score.

To support the visualization of the dataset have developed a web visualization tool using the ViSUS WebViewer (www.visus.org) to allow users to view all of the trees at the full site scale with the ability to zoom and pan to examine individual groups of trees down to a scale of 20m (see http://visualize.idtrees.org, Figure 2). This tool will allow the ecological community to assist in identifying areas in need of further refinement within the over 500,000 ha of area covered by the 37 sites.

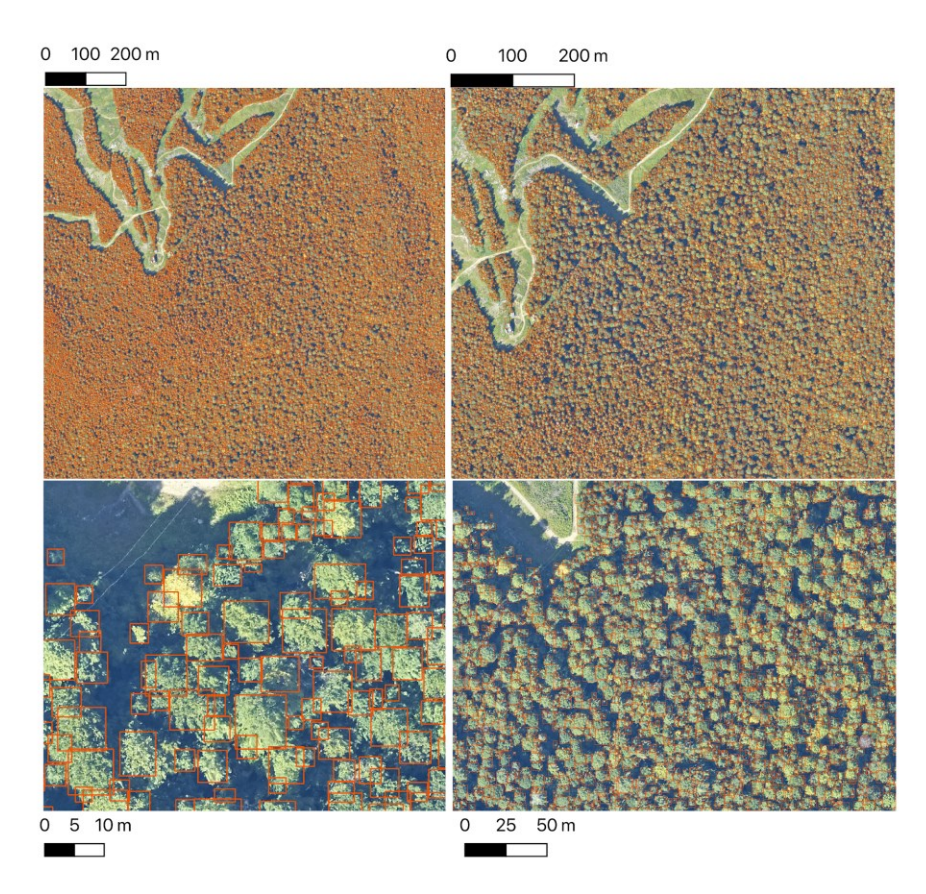


Figure 2. The Neon Crowns Dataset provides individual-level tree predictions at broad scales. An example from Bartlett Forest, NH shows the ability to continuously zoom from landscape level to stand level views.

Crown Delineation Methods

The location of individual tree crowns was estimated using a semi-supervised deep learning workflow (Figure 3; [6,7]). This workflow uses a one-shot object detector with a convolutional neural network backbone to identify trees in RGB imagery. The model was pre-trained using weak labels generated from a previous published LiDAR tree detection algorithm using NEON data from 30 sites [8]. The model was then trained on 10,000 hand-annotated crowns from 7

NEON sites (Figure 1). This phase of the workflow was performed using the DeepForest python package [9]. We extend the workflow by filtering trees using the LiDAR-derived canopy height model to remove objects identified by the model with heights of <3m (Supplementary Material). This addition was important in sparsely vegetated landscapes, such as oak savannah and deserts where it was difficult for the model to distinguish between trees and low shrubs in the RGB imagery.

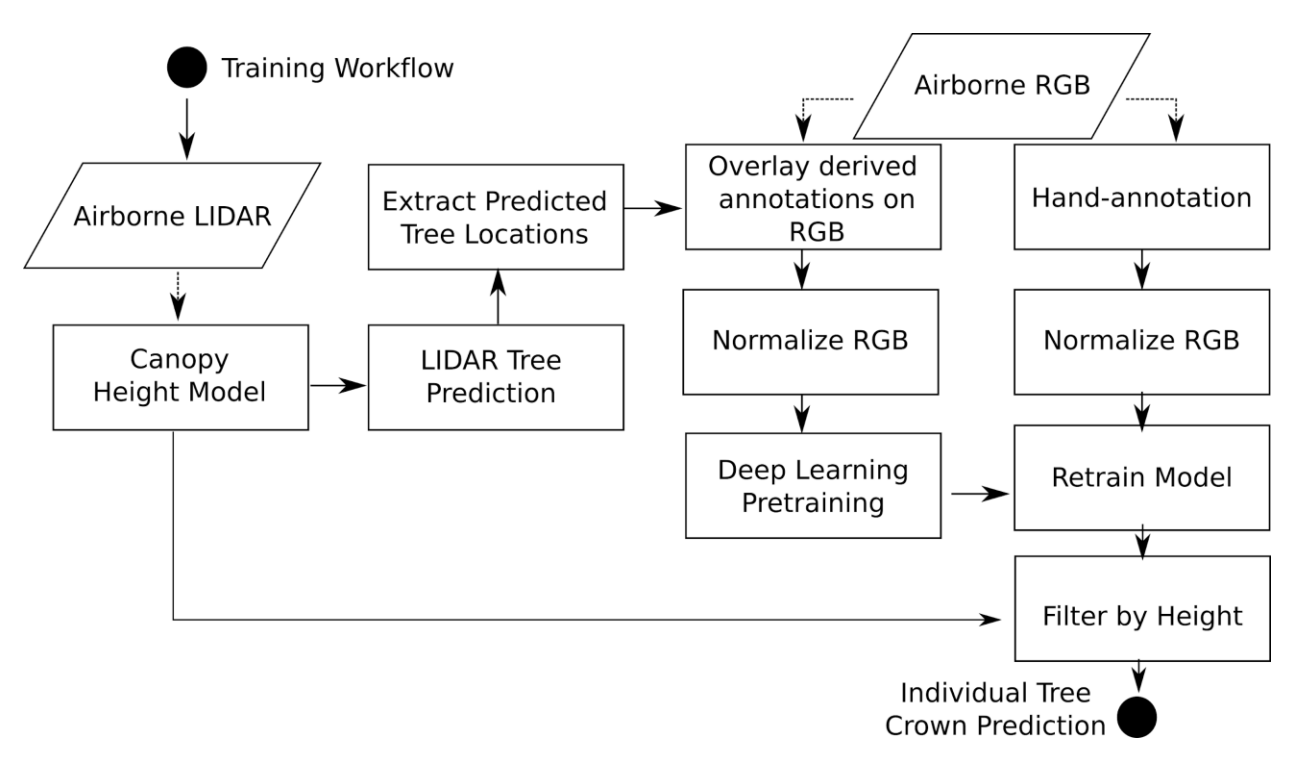


Figure 3. Workflow diagram adapted from [9]. The workflow for model training and development are identical to [9] with the exception of extracting heights from the canopy height model for each bounding box prediction.

Evaluation and Validation

Building on evaluation methods from [6,7,9], we validated the dataset using hand-annotated bounding boxes drawn by an observer looking directly at the sensor data. We refer to this type of evaluation data as 'image-annotated crowns'. This approach allows the performance of the crown-delineation algorithm to be evaluated across the full range of forest types represented in the continental-scale dataset. However, note that these image-annotated crowns will not be as accurate as field-annotated crowns [10], and therefore may overestimate the performance of the algorithm relative to true ground truth.

We compared predicted tree crowns to image-annotated crowns from 21 NEON sites (n=207 images, 6926 trees) that were withheld from model training. These sites were selected to cover a wide range of forest types and geographies. Using a 50% intersection over union threshold, our workflow yielded a bounding box recall of 72.4% with a precision of 70.5%. Recall is the proportion of image-annotated crowns matched to a crown prediction and precision is the

proportion of predictions that match image-annotated crowns. Precision and recall are equally important for developing a tree crown dataset, because it is important to both successfully identify trees and ignore non-tree objects. Tests indicate that the model generalizes well across geographic sites and forest conditions (Figure 4; [6,9]), but there is a general bias towards undersegmenting trees in dense stands where multiple individual trees with similar optical characteristics are grouped into a single delineation. Additional training data and the LiDAR threshold added in this implementation resulted in predictions that were 4.1% more precise, but 2.8% less accurate than [9] (Figure 4). The decrease in recall likely occurs because the NEON field plots that were used for evaluation occur mostly in forested areas of the NEON sites, rather than in less dense areas of the sites. Areas with less dense forest (e.g., agriculture, suburban areas, and bare ground) are not as common within the NEON field plots used for evaluation and are likely the areas with improved precision from the use of the new LiDAR threshold (Supplementary Material). The 4% increase in precision is therefore likely a lower bound and is worth the trade-off in the minimal drop in recall.

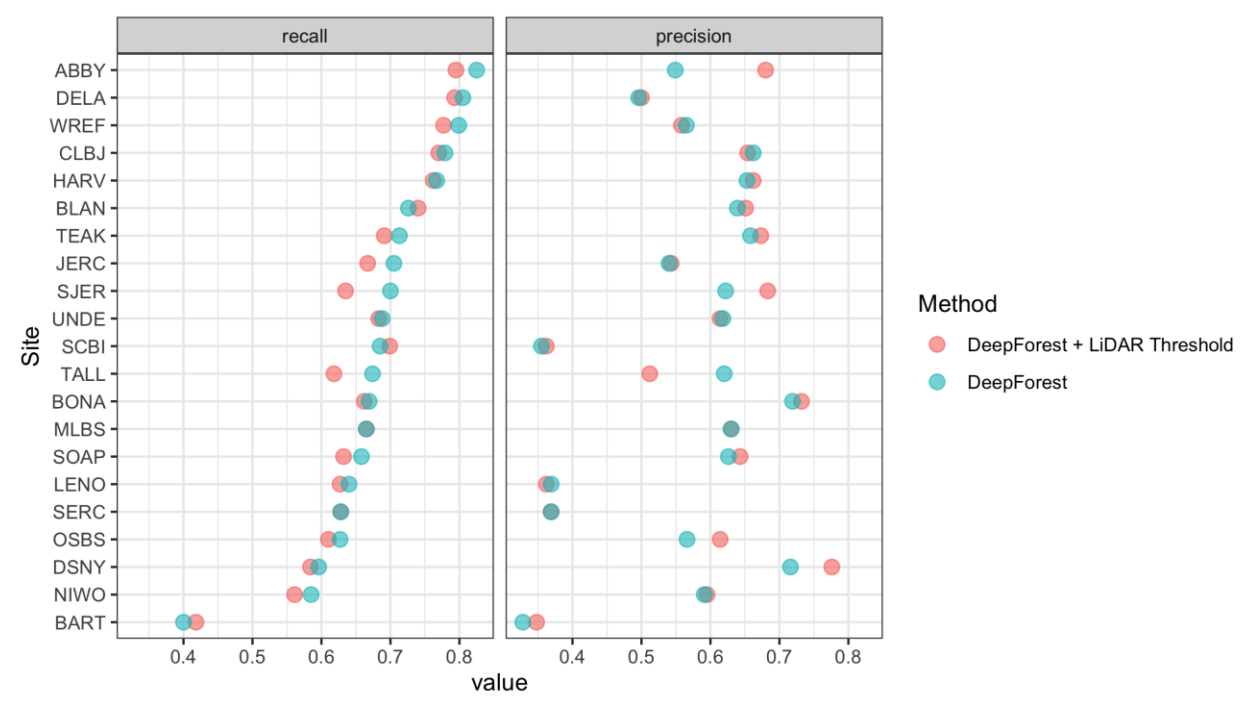


Figure 4. Precision and recall scores for the algorithm used to create the NEON Crowns Dataset (red points), as well as the DeepForest model from [9] (blue points). Evaluation is performed on 207 image-annotated images (6926 trees) in the NEONTreeEvaluation dataset (https://github.com/weecology/NeonTreeEvaluation).

We also compared crowns delineated by the algorithm to field-collected stems from NEON's Woody Vegetation Structure dataset. This data product contains a single point for each tree with a stem diameter ≥ 10cm. We filtered the raw data to only include trees likely to be visible in the canopy (see Appendix S1). These overstory tree field data help us analyze the performance of our workflow in matching crown predictions to individual trees by scoring the proportion of field stems that fall within a prediction. Field stems can only be applied to one

prediction, so if two predictions overlap over a field stem, only one is considered a positive match. This test produces an overall stem recall rate at 69.4%, similar to the bounding box recall rate from the image-annotated data (Figure 5). The analysis of stem recall rate is conservative due to the challenge of aligning the field-collected spatial data with the remote sensing data (Appendix S1). We found several examples of good predictions that were counted as false positives due to errors in the position of the ground samples within the imagery.

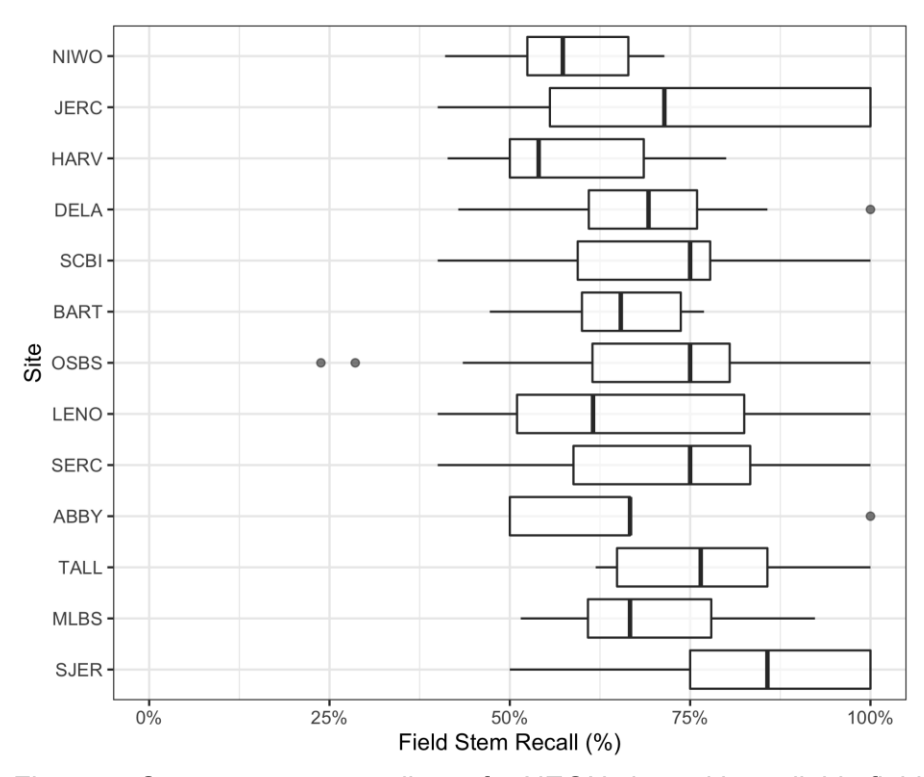


Figure 5. Overstory stem recall rate for NEON sites with available field data. Each data point is the recall rate for a field-collected plot. NEON plots are either 40mx40m 'tower' plots with two 20x20m subplots, or a single 20mx20m 'distributed' plot. See NEON sampling protocols for details. For site abbreviations see S3.

To assess the utility of our approach for mapping forest structure, we compared remotely sensed predictions of maximum tree height to field measurements of tree height of overstory trees using NEON's Woody Plant Vegetation Structure Data. We used the same workflow described in Appendix S1 for determining overstory status for both the stem recall and height verification analysis. Predicted heights showed good correspondence with field-measured heights of reference trees. Using a linear-mixed model with a site-level random effect, the predicted crown height had a Root Mean Squared Error of 1.73m (Figure 6). The relationship is stronger in forests with more open canopies (SJER, OSBS) and predictably more prone to error in forests with denser canopies (BART, MLBS). Given the challenges of measuring tree heights, including the difficulty of measuring tree height in the field, the potential for tree growth between the time of field measurement and image acquisition (often several years), and the automated

workflow to designate whether field-collected trees were visible in the canopy, these results suggest that overstory height measures are reasonably accurate across the dataset.

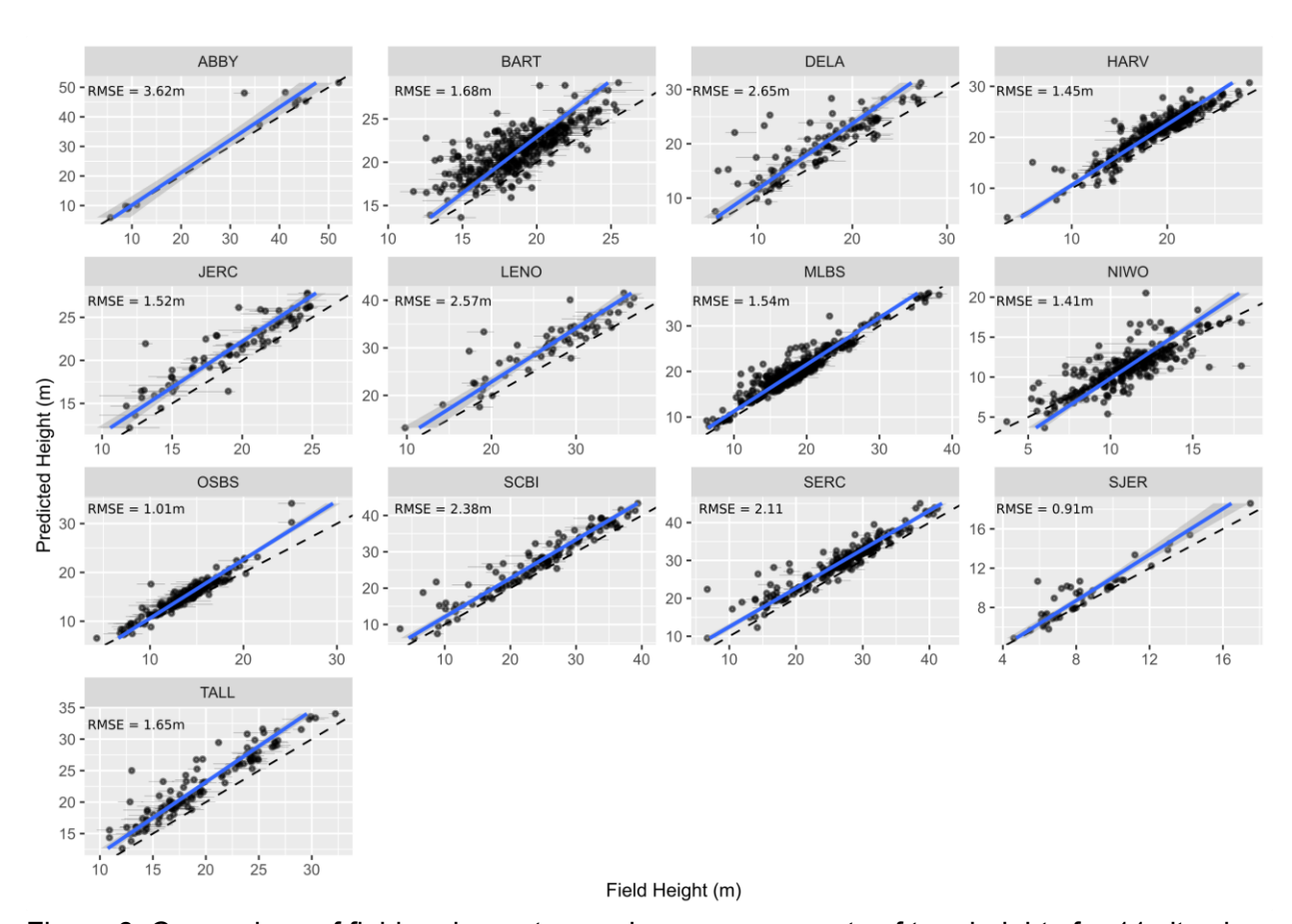


Figure 6. Comparison of field and remote sensing measurements of tree heights for 11 sites in the National Ecological Observatory Network. Each point is an individual tree. See text and S1 for selection criteria and matching scheme for the field data. The RMSE of a mixed-effects model with a site level random effect is 1.73m.

Using the NEON Crowns dataset for individual, landscape and biogeographic scale applications

This dataset supports individual-level cross-scale ecological research that has not been previously possible. It provides the unique combination of information spanning the entire United States, with sites ranging from Puerto Rico to Alaska, with continuous individual-level data within sites at scales hundreds of times larger than what is possible using field-based survey methods. At the individual level, high-resolution airborne imagery can inform analysis of critical forest properties, such as tree growth and mortality [11], foliar biochemistry [12], and landscape-scale carbon storage [13]. Because field data on these properties are measured on individual trees, individual level tree detection allows connecting field data directly to image data. In addition, growth, mortality and changes in carbon storage occur on the scale of individual trees such that detection of individual crowns allows direct tracking of these properties

across space and time. While it is possible to aggregate information at the stand level, we believe that individual level data opens new possibilities in large scale forest monitoring and provides richer insights into the underlying mechanisms that drive these patterns.

At landscape scales, research is often focused on the effect of environmental and anthropogenic factors on forest structure and biodiversity. For example, understanding why tree abundance and biomass vary across landscapes has direct applications to numerous ecological questions and economic implications(e.g. [14]). Often, this requires sampling at a number of disparate locations and either extrapolation to continuous patterns at landscape scales, or assumptions that the range of possible states of the system are captured by the samples. Using the individual level data from this dataset, we can now produce continuous high resolution maps across entire NEON sites for enabling landscape scale studies of multiple ecological phenomena (Figure 7). These landscape scale responses can then be combined with high resolution data on natural and anthropogenic drivers (e.g., topography, soils, fire management) to model forest dynamics at broad scales.

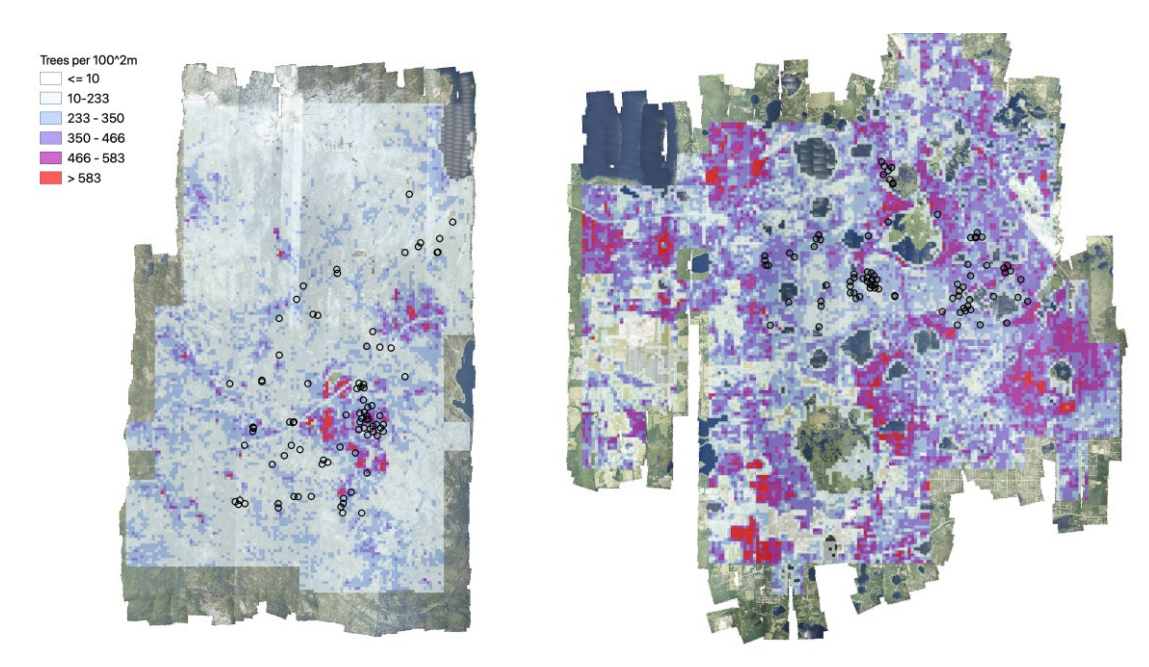


Figure 7. Tree density maps for Teakettle Canyon, California (left) and Ordway Swisher Biological Station, Florida (right). For each 100m^2 pixel, the total number of predicted crowns were counted. The location of NEON Woody Plant Vegetation sampling plots are shown in black circles.

By focusing on detecting individual trees, this approach to landscape scale forest analysis does not require assumptions about spatial similarity, sufficiently extensive sampling, or consistent responses of the ecosystem to drivers across spatial gradients. This is important because the heterogeneity of forest landscapes makes it difficult to use field plot data on quantities such as tree density and biomass to extrapolate inference to broad scales [15]. To illustrate this challenge, we compared field-measured tree densities of NEON field plots to estimated densities of 10,000 remotely sensed plots of the same size placed randomly

throughout the landscapes across footprints of the airborne data. We attempted to change the Woody Vegetation data as little as possible (i.e. compared to the more refined filtered data in previous analyses) in order to obtain estimates of tree cover in a plot from the field data. To be included in this analysis, trees needed to have valid spatial coordinates and a minimum height of 3m. Some older data lacked height estimates, in which case we used a minimum dbh threshold of 15cm for inclusion. In each simulated plot, we then counted the total number of predicted tree crowns to create a distribution of tree densities at the site level (Figure 8). Comparing the field plot tree densities with the distribution from the full site shows deviations for most sites, with NEON field plots exhibiting higher tree densities than encountered on average in the airborne data for some sites (e.g., Teakettle Canyon, CA) and lower tree densities than from remote sensing in others (e.g., Ordway-Swisher Biological Station). While this kind of comparison is inherently difficult due to differing thresholds and filters for data inclusion in field versus remotely sensed data, but highlights that even well stratified sampling of large landscapes as was done with NEON plots (see NEON technical documents for NEON.DP1.10098) can produce differing tree attribute estimates than continuous sampling from remote sensing data. Combining representative field sampling with remote sensing to produce data products like the NEON Crowns dataset provides an approach to addressing this challenge to improve estimations of the abundance, biomass, and size distributions across large geographic areas.

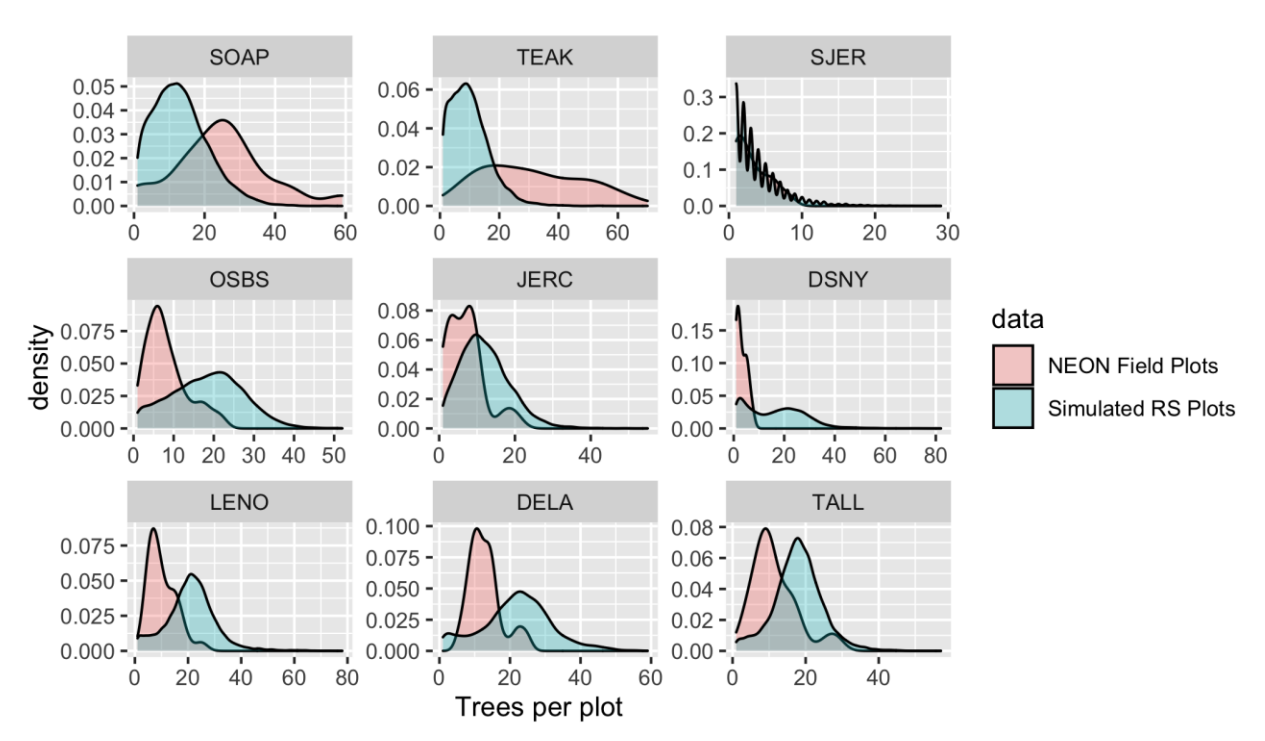


Figure 8. Comparison of tree counts between the field-collected NEON plots and the predicted plots from the crowns dataset. For the remote sensing data, 10000 simulated 40m² plots were calculated for each site for the full AOP footprint for each year. To mimic NEON sampling, 2 quadrants were randomly sampled in each simulated plot. No plots on water, bare ground, or herbaceous land classes were included in the comparison. We selected three sites from three

NEON domains to show a sample of sites across the continental US. Both distributed and tower NEON plots were used for these analyses.

The NEON Crowns dataset supports the assessment of cross-site patterns to help understand the influence of large scale processes on forest structure at biogeographic scales. For example, ecologists are interested in how and why forest characteristics such as abundance, biomass, and allometric relationships vary among forest types (e.g. [16]) and how these patterns covary across environmental gradients [17]. Understanding these relationships is important for inferring controls over forest stand structure, understanding individual tree biology, and assessing stand productivity. By providing standardized data that span near-continental scales, this dataset can help inform the fundamental mechanisms that shape forest structure and dynamics. For example, we can calculate tree allometries (e.g., the ratio of tree height to crown area) on a large number of individual trees across NEON sites and explore how allometry varies with stand density and vegetation type (Figure 9). This example analysis shows a continental-scale relationship, with denser forests exhibiting trees with narrower crowns for the same tree height compared to less dense forests, but also clustering and variation in the relationship within vegetation types. For example, subalpine forests illustrate relationships between tree density and allometry that are distinct from other forest types. By defining both general biogeographic patterns, and deviations therein, this dataset will allow the investigation of factors shaping forest structure at macroecological scales.

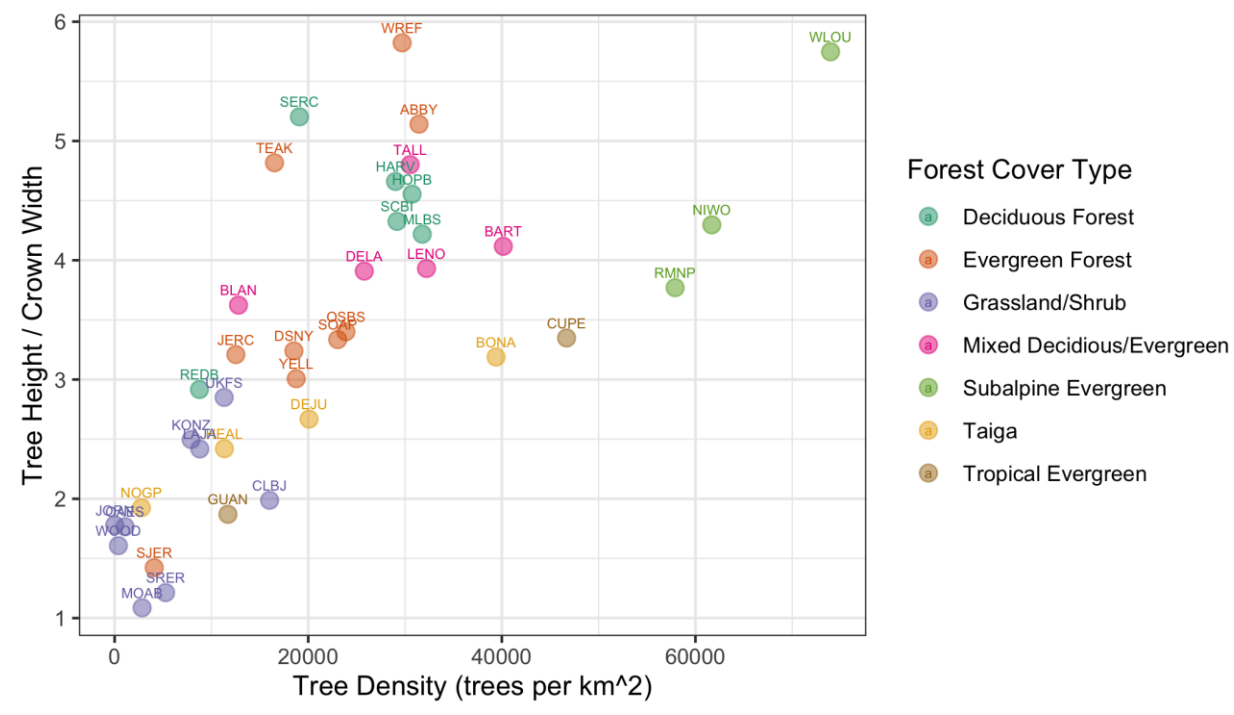


Figure 9. Individual crown attributes for predictions made at each NEON site. For site abbreviations see S1. Crown area is calculated by multiplying the width and height of the predicted crown bounding box. Crown height is the 99th quantile of the LiDAR returns that fall inside the predicted crown bounding box. Sites are colored by the dominant forest type to illustrate the general macroecological relationship among sites in similar biomes.

In addition to these ecological applications, the NEON Crowns dataset can also act as a foundation for other machine learning and computer vision applications in forest informatics, such as tree health assessments, species classification, or foliar trait estimation. In each of these tasks, individual tree delineation is the first step to associate sensor data with ground measurements. However, delineation requires a distinct set of technical background and computational approaches and thus many ecological applications either skip an explicit delineation step entirely [18] or apply existing software without detailed exploration of segmentation performance (e.g. [19]). Ignoring these factors can hamper accurate assessments due to mismatches between sensor data and individuals. While our crown annotations are not perfect, they are specifically tailored to one of the largest and openly accessible datasets that allows pairing individual tree detections with information on species identity, tree health, and leaf traits through NEONs field sampling, and we believe they are sufficiently robust to serve as the basis for broad scale analysis.

Limitations and Further Technical Developments

An important limitation for this dataset is that it only provides information on sun-exposed tree crowns. It is therefore not appropriate for ecological analyses that depend on accurate characterization of subcanopy trees and the three-dimensional structure of forest stands. Fortunately, a number of the major questions and applications in ecology are primarily influenced by large individuals [20]. For example, biomass estimation is largely driven by the canopy in most ecosystems, rather than mid or understory trees that are likely to be missed by aerial surveys. Similarly, habitat classification and species abundance curves can depend on the dominant forest structure that can be inferred from coarse resolution airborne data [21] and could be improved using this dataset. It may be possible to establish relationships between understory and canopy measures using field data that could allow this dataset to be used as part of a broader analysis [22]. However, this would require significant additional research to validate the potential for this type of approach.

An additional limitation is the uncertainty inherent in the algorithmic detection of crowns. While we found good correspondence between image-based crown annotations and those produced by the model for many sites, there remained substantial uncertainty across all sites and reasonable levels of error in some sites. It is important to consider how this uncertainty will influence the inference from research using this and similar datasets. The model is biased towards undersegmentation, meaning that multiple trees are prone to being grouped as a single crown. It is also somewhat conservative in estimating crown extent wherein it tends to ignore small extensions of branches from the main crown. These biases could impact studies of tree allometry and biomass if the analysis is particularly sensitive to crown area. When making predictions for ecosystem features such as biomass, it will be important to propagate the uncertainty in individual crowns into downstream analyses. While confidence scores for individual detections are provided to aid uncertainty propagation, the use of additional ground truth data may also be necessary to infer reliability.

One aspect of individual crown uncertainty that we have not addressed is the uncertainty related to image-based crown annotations and measurement of trees in the field [10]. To allow

training and evaluating the model across a broad range of forest types, we used image-based crown annotations. This approach assumes that crowns identifiable in remotely sensed imagery accurately reflect trees on the ground. This will not always be the case, as what appears to be a single crown from above may constitute multiple neighboring trees, and conversely, what appears to be two distinct crowns in an image may be two branches of a single large tree [10]. Targeted field surveys will be always needed to validate these predictions and community annotation efforts will allow for assessment of this component of uncertainty.

The machine learning workflow used to generate this dataset also has several areas that could be improved for greater accuracy, transferability and robustness. The current model contains a single class 'Tree' with an associated confidence score. This binary representation prevents the model from differentiating between objects that are not trees and objects for which sufficient training information is not available. For example, the model has been trained to ignore buildings and other vertical structures that may look like trees. However, when confronted by objects data that has never been encountered, it often produces unintuitive results. Examples of objects that did not appear in the training data, and as a result were erroneously predicted as trees, include weather stations, floating buoys, and oil wells. Designing models that can identify outliers, anomalies, and 'unknown' objects is an active area of research in machine learning [] and will be useful in increasing accuracy in novel environments. Also, NEON data can sometimes be afflicted by imaging artifacts due to co-registration issues with LiDAR and raw RGB imagery (Appendix S2). This effect can lead to distorted imagery that appears fuzzy and swirled and lead to poor segmentation. An ideal model would detect these areas of poor quality and label them as 'unknown' rather than attempting to detect trees in these regions.

Given these limitations, we view this version of the dataset as the first step in an iterative process to improve cross-scale individual level data on trees. Ongoing assessment of these predictions using both our visualization tool and field-based surveys will be crucial to continually identify areas for improvements in both training data and modeling approaches. While iterative improvements are important, the accuracy of the current predictions illustrates that this dataset is sufficiently precise for addressing many cross-scale questions related to forest structure. By providing broad scale crown data we hope to highlight the promising integration between deep learning, remote sensing, and forest informatics, and provide access to the results of this next key step in ecological research to the broad range of stakeholders who can benefit from these data.

Acknowledgements

We would like to thank NEON staff and in particular Tristan Goulden and Courtney Meier for their assistance and support. This research was supported by the Gordon and Betty Moore Foundation's Data-Driven Discovery Initiative (GBMF4563) to E.P. White and by the National Science Foundation (1926542) to E.P. White, S.A. Bohlman, A. Zare, D.Z. Wang, and A. Singh. The funders had no role in study design, data collection and analysis, decision to publish, or preparation of the manuscript.

Literature Cited

- 1. Crowther TW, Glick HB, Covey KR, Bettigole C, Maynard DS, Thomas SM, et al. Mapping tree density at a global scale. Nature. 2015;525: 201–205. doi:10.1038/nature14967
- 2. Hansen MC, Potapov PV, Moore R, Hancher M, Turubanova SA, Tyukavina A, et al. High-Resolution Global Maps of 21st-Century Forest Cover Change. Science. 2013;342: 850–853. doi:10.1126/science.1244693
- 3. Bastin J-F, Rutishauser E, Kellner JR, Saatchi S, Pélissier R, Hérault B, et al. Pan-tropical prediction of forest structure from the largest trees. Glob Ecol Biogeogr. 2018;27: 1366–1383. doi:10.1111/geb.12803
- 4. Puliti S, Breidenbach J, Astrup R. Estimation of Forest Growing Stock Volume with UAV Laser Scanning Data: Can It Be Done without Field Data? Remote Sens. 2020;12: 1245. doi:10.3390/rs12081245
- Aubry-Kientz M, Dutrieux R, Ferraz A, Saatchi S, Hamraz H, Williams J, et al. A Comparative Assessment of the Performance of Individual Tree Crowns Delineation Algorithms from ALS Data in Tropical Forests. Remote Sens. 2019;11: 1086. doi:10.3390/rs11091086
- 6. Weinstein BG, Marconi S, Bohlman SA, Zare A, White EP. Cross-site learning in deep learning RGB tree crown detection. Ecol Inform. 2020;56: 101061. doi:10.1016/j.ecoinf.2020.101061
- 7. Weinstein BG, Marconi S, Bohlman S, Zare A, White E. Individual Tree-Crown Detection in RGB Imagery Using Semi-Supervised Deep Learning Neural Networks. Remote Sens. 2019;11: 1309. doi:10.3390/rs11111309
- 8. Silva CA, Hudak AT, Vierling LA, Loudermilk EL, O'Brien JJ, Hiers JK, et al. Imputation of Individual Longleaf Pine (*Pinus palustris* Mill.) Tree Attributes from Field and LiDAR Data. Can J Remote Sens. 2016;42: 554–573. doi:10.1080/07038992.2016.1196582
- 9. Weinstein BG, Marconi S, Aubry-Kientz, Mélaine M, Vincent G, Senyondo H, White E. DeepForest: A Python package for RGB deep learning tree crown delineation. Methods Ecol Evol. 2020.
- 10. Graves S, Gearhart J, Caughlin TT, Bohlman S. A digital mapping method for linking high-resolution remote sensing images to individual tree crowns. PeerJ Preprints; 2018 Sep. doi:10.7287/peerj.preprints.27182v1
- 11. Clark DB, Castro CS, Alvarado LDA, Read JM. Quantifying mortality of tropical rain forest trees using high-spatial-resolution satellite data. Ecol Lett. 2004;7: 52–59. doi:10.1046/j.1461-0248.2003.00547.x
- 12. Chadwick KD, Asner GP. Organismic-Scale Remote Sensing of Canopy Foliar Traits in Lowland Tropical Forests. Remote Sens. 2016;8: 87. doi:10.3390/rs8020087
- 13. Graves SJ, Caughlin TT, Asner GP, Bohlman SA. A tree-based approach to biomass estimation from remote sensing data in a tropical agricultural landscape. Remote Sens Environ. 2018;218: 32–43. doi:10.1016/j.rse.2018.09.009
- 14. Laubhann D, Sterba H, Reinds GJ, De Vries W. The impact of atmospheric deposition and climate on forest growth in European monitoring plots: An individual tree growth model. For Ecol Manag. 2009;258: 1751–1761. doi:10.1016/j.foreco.2008.09.050
- 15. Marvin DC, Asner GP, Knapp DE, Anderson CB, Martin RE, Sinca F, et al. Amazonian landscapes and the bias in field studies of forest structure and biomass. Proc Natl Acad Sci. 2014;111: E5224–E5232. doi:10.1073/pnas.1412999111
- 16. Jucker T, Caspersen J, Chave J, Antin C, Barbier N, Bongers F, et al. Allometric equations for integrating remote sensing imagery into forest monitoring programmes. Glob Change Biol. 2017;23: 177–190. doi:10.1111/gcb.13388
- 17. Feldpausch TR, Banin L, Phillips OL, Baker TR, Lewis SL, Quesada CA, et al. Height-

- diameter allometry of tropical forest trees. Biogeosciences. 2011;8: 1081–1106. doi:10.5194/bg-8-1081-2011
- 18. Williams J, Schönlieb C-B, Swinfield T, Irawan B, Achmad E, Zudhi M, et al. SLIC-UAV: A Method for monitoring recovery in tropical restoration projects through identification of signature species using UAVs. ArXiv200606624 Cs Stat. 2020 [cited 24 Aug 2020]. Available: http://arxiv.org/abs/2006.06624
- 19. Maschler J, Atzberger C, Immitzer M. Individual Tree Crown Segmentation and Classification of 13 Tree Species Using Airborne Hyperspectral Data. Remote Sens. 2018;10: 1218. doi:10.3390/rs10081218
- 20. Enquist BJ,, Yadvinder M, et al. The megabiota are disproportionately important for biosphere functioning. Nat Commun Lond. 2020;11. doi:http://dx.doi.org.lp.hscl.ufl.edu/10.1038/s41467-020-14369-y
- 21. Shirley SM, Yang Z, Hutchinson RA, Alexander JD, McGarigal K, Betts MG. Species distribution modelling for the people: unclassified landsat TM imagery predicts bird occurrence at fine resolutions. Divers Distrib. 2013;19: 855–866. doi:10.1111/ddi.12093
- 22. Bohlman SA. Species Diversity of Canopy Versus Understory Trees in a Neotropical Forest: Implications for Forest Structure, Function and Monitoring. Ecosystems. 2015;18: 658–670. doi:10.1007/s10021-015-9854-0

Supplemental Materials

S1. Evaluation of the workflow on NEON collected field stems

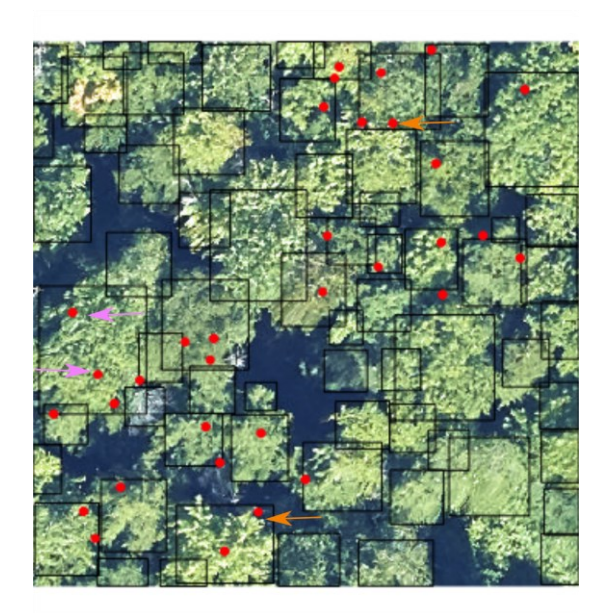
Raw NEON tree stem data was processed from the NEON data portal to provide a data set to compare image derived heights to field measured heights. The following filters were applied to the raw NEON field data (ID: DP1.10098.001) after download. A reference tree must have

- Valid spatial coordinates
- A unique height measurement per sampling period. Individuals double recorded but with different heights were discarded
- Height measurements in more than one year to verify height measurement
- Changes in between-year field heights of less than 6m
- A classification as alive
- A minimum height of 3m to match the threshold in the remote sensing workflow.
- Be at least within 5m of the canopy as measured by the LiDAR height model extracted at the stem location. This was used to prevent matching with understory trees in the event that overstory trees were eliminated due to failing in one of the above conditions, or not sampled by NEON.

To match trees in the field and the NEON Crowns dataset, we took the closest height when two predictions and field stems overlapped. We also dropped CLBJ since only 3 points met this criteria. All other NEON sites did not have any data that met this criteria.



Figure S5. Example stem recall for evaluation plot JERC_048 from Jones Ecological Resource Center, Georgia. Predicted tree bounding boxes in black. Filtered NEON field stems (see above for filtering criteria) in red.



S6. Example from NEON plot BART_050 from Bartlett Forest, New Hampshire. In dense forests, multiple field stems can fall within a single predicted bounding box. This is due to both under-segmentation of visible crowns (pink arrows), as well as potentially incomplete filtering of field stems to identify overstory trees visible in the image (orange arrows).

Figure S5 and Figure S6 highlight some of the challenges of matching remote sensing crown predictions and field collected stem data. In Figure S5, the green arrow shows the simplest scenario, a single prediction unambiguously overlaps a single collected stem. The black arrow shows a moderately challenging scenario in which a visually unambiguous crown only barely matches the field collected stem. This could occur due 1) the stem growing at an angle leading

to a spatial mismatch between crown and stem, 2) spatial error in measuring the crown location, 3) spatial error in the georeferencing of the RGB image. The blue arrow shows a stem point that does not overlap with a prediction crown. We have written the stem recall evaluation to be conservative, allowing no tolerance for points outside of the prediction box. Therefore, the stem recall for this image was 4/6 = 66.66%, which we believe is a conservative representation of the performance of the algorithm given the uncertainty in the field data and matching process.

S2. Qualitative Assessment of Broad Scale Predictions

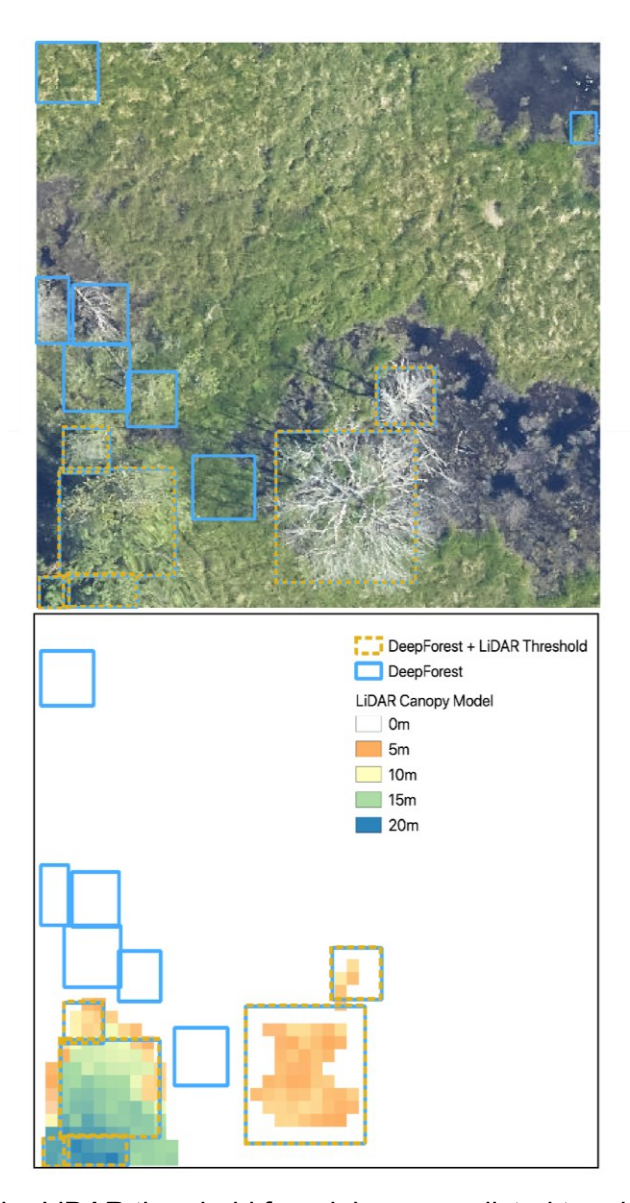


Figure 4. Illustration of the LiDAR threshold for minimum predicted tree height using NEON plot ID OSBS_023 from Ordway Swisher Biological Station, Florida. Using the DeepForest algorithm [9], in blue, several boxes were removed based on no LiDAR returns above 3m (dotted orange). This step was key in open-ground areas in which the algorithm can confuse short vegetation with standing trees.

With over 7,000 1km2 tiles, it is not possible to do a systematic check of predicted crowns. Our aim is to provide users with a broad scale description of areas of concern. There are two main types of failure modes, data quality and algorithm quality. Data quality errors can occur in either the RGB data or LiDAR products. RGB errors include incomplete site coverage,

image artifacts due to georectification, errors in orthomosaic stitching and lighting changes among data collection events (Figure S6).

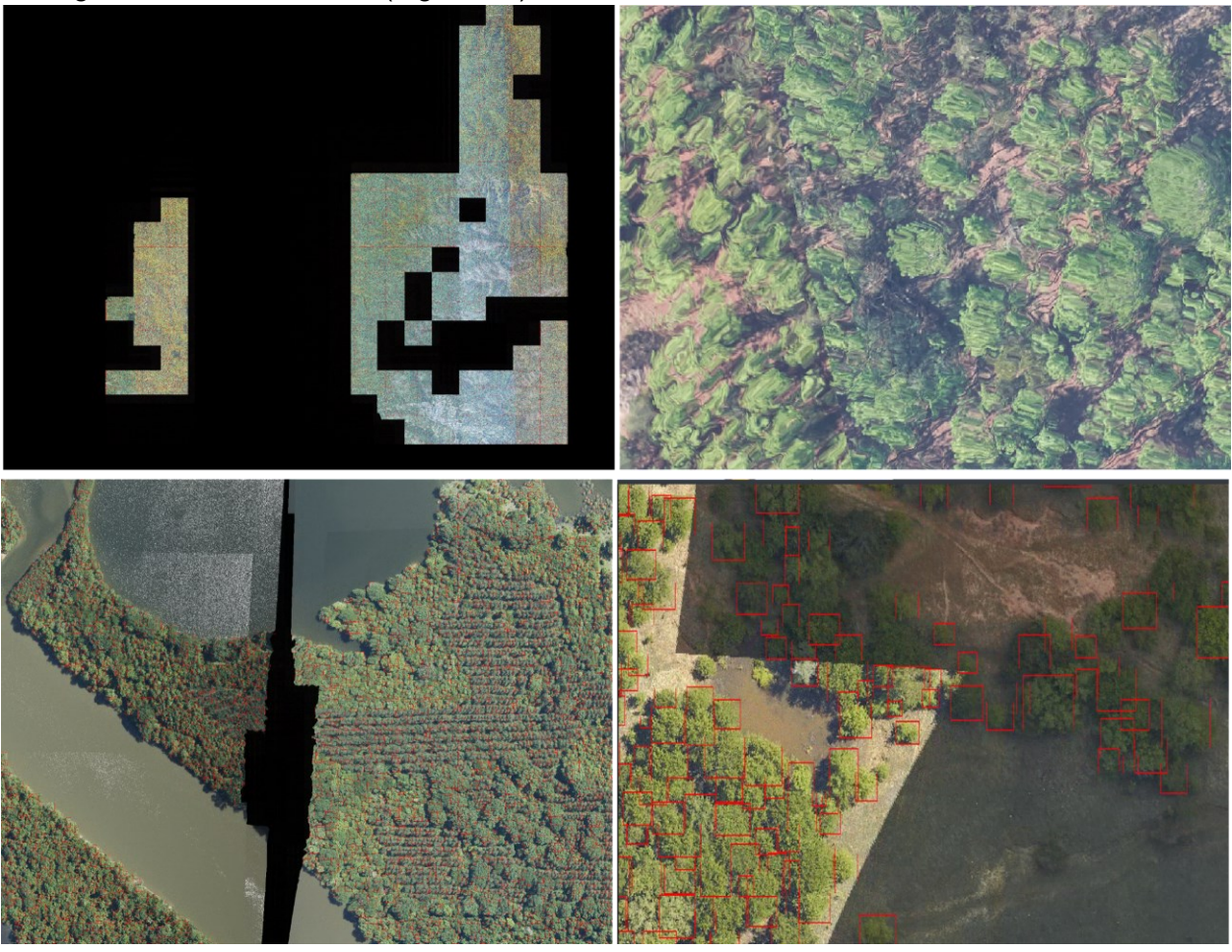


Figure S6. Errors in data quality leading to inaccurate predictions or inappropriate use cases. Top left) Patchy coverage at the site level can prevent broad scale analysis with large gaps in RGB data availability (NEON site GRSM). Top right) RGB artifacts at the edge of images stem from the challenge of georectification of the RGB and LiDAR tiles leading to swirling in the RGB pixels (NEON site OSBS). Bottom left) Seams in the flightlines in the RGB images leads to gaps in local predictions (NEON site DELA). Bottom right) Changes in illumination among data acquisition collections lead to stark changes in pixel values.

S3. NEON Site Abbreviations

		Domain			
Site Name	siteID	Number	State	Latitude	Longitude

Abby Road	ABBY	D16	WA	45.76243	-122.33033
Bartlett Experimental Forest	BART	D01	NH	44.06388	-71.28731
Blandy Experimental Farm	BLAN	D02	VA	39.06026	-78.07164
Caribou-Poker Creeks Research Watershed	BONA	D19	AK	65.15401	-147.50258
watershed	BOWA		7410	03.13401	147.30230
LBJ National Grassland	CLBJ	D11	TX	33.40123	-97.57
Rio Cupeyes	CUPE	D04	PR	18.11352	-66.98676
Delta Junction	DEJU	D19	AK	63.88112	-145.75136
Dead Lake	DELA	D08	AL	32.54172	-87.80389
Disney Wilderness Preserve	DSNY	D03	FL	28.12504	-81.4362
Guanica Forest	GUAN	D04	PR	17.96955	-66.8687
Harvard Forest	HARV	D01	MA	42.5369	-72.17266
Healy	HEAL	D19	AK	63.87569	-149.21334

Lower Hop Brook	НОРВ	D01	MA	42.47179	-72.32963
Jones Ecological Research Center	JERC	D03	GA	31.19484	-84.46861
Jornada LTER	JORN	D14	NM	32.59068	-106.84254
JOHNAU ETEK	301114	D14	INIVI	32.33000	100.04254
Konza Prairie Biological Station	KONZ	D06	KS	39.10077	-96.56309
Lajas Experimental Station	LAJA	D04	PR	18.02125	-67.0769
Lenoir Landing	LENO	D08	AL	31.85388	-88.16122
Mountain Lake Biological Station	MLBS	D07	VA	37.37828	-80.52484
Moab	MOAB	D13	UT	38.24833	-109.38827
Niwot Ridge Mountain Research					
Station	NIWO	D13	СО	40.05425	-105.58237
Northern Great Plains Research					
Laboratory	NOGP	D09	ND	46.76972	-100.91535
Klemme Range Research Station	OAES	D11	ОК	35.41059	-99.05879
Ordway-Swisher Biological Station	OSBS	D03	FL	29.68927	-81.99343

Red Butte Creek	REDB	D15	UT	40.78374	-111.79765
Rocky Mountain National Park, CASTNET	RMNP	D10	СО	40.27591	-105.54592
Smithsonian Conservation Biology Institute	SCBI	D02	VA	38.89292	-78.1395
Smithsonian Environmental Research Center	SERC	D02	MD	38.89008	-76.56001
San Joaquin Experimental Range	SJER	D17	CA	37.10878	-119.73228
Soaproot Saddle	SOAP	D17	CA	37.03337	-119.26219
Santa Rita Experimental Range	SRER	D14	AZ	31.91068	-110.83549
Talladega National Forest	TALL	D08	AL	32.95046	-87.39327
Lower Teakettle	TEAK	D17	CA	37.00583	-119.00602
West St Louis Creek	WLOU	D13	СО	39.89137	-105.9154
Woodworth	WOOD	D09	ND	47.12823	-99.24136
Wind River Experimental Forest	WREF	D16	WA	45.82049	-121.95191

Yellowstone Northern Range (Frog					
Rock)	YELL	D12	WY	44.95348	-110.53914